Debris and Radiation-Induced Damage Effects on EUV Nanolithography Source Collector Mirror Optics Performance

J. P. Allain*, M. Nieto, M. Hendricks, S.S. Harilal, A. Hassanein

Argonne National Laboratory, Argonne, Illinois

ABSTRACT

Exposure of collector mirrors facing the hot, dense pinch plasma in plasma-based EUV light sources to debris (fast ions, neutrals, off-band radiation, droplets) remains one of the highest critical issues of source component lifetime and commercial feasibility of nanolithography at 13.5-nm. Typical radiators used at 13.5-nm include Xe and Sn. Fast particles emerging from the pinch region of the lamp are known to induce serious damage to nearby collector mirrors. Candidate collector configurations include either multi-layer mirrors (MLM) or single-layer mirrors (SLM) used at grazing incidence.

Studies at Argonne have focused on understanding the underlying mechanisms that hinder collector mirror performance at 13.5-nm under fast Sn or Xe exposure. This is possible by a new state-of-the-art *in-situ* EUV reflectometry system that measures real time relative EUV reflectivity (15-degree incidence and 13.5-nm) variation during fast particle exposure. Intense EUV light and off-band radiation is also known to contribute to mirror damage. For example off-band radiation can couple to the mirror and induce heating affecting the mirror's surface properties. In addition, intense EUV light can partially photo-ionize background gas (e.g., Ar or He) used for mitigation in the source device. This can lead to local weakly ionized plasma creating a sheath and accelerating charged gas particles to the mirror surface and inducing sputtering.

In this paper we study several aspects of debris and radiation-induced damage to candidate EUVL source collector optics materials. The first study concerns the use of IMD simulations to study the effect of surface roughness on EUV reflectivity. The second studies the effect of fast particles on MLM reflectivity at 13.5-nm. And lastly the third studies the effect of multiple energetic sources with thermal Sn on 13.5-nm reflectivity. These studies focus on conditions that simulate the EUVL source environment in a controlled way.

Keywords: threshold sputtering, EUV reflectivity, multi-layer mirror, EUV collector optics, X-ray reflectivity, Sn debris

1. INTRODUCTION

One of the leading factors reducing lifetime and performance of EUV mirrors in EUV lithography sources based on Sn-plasma is contamination by condensed thermal Sn particles and energetic Sn. These contaminants emanate from the pinch plasma in discharge and laser produced plasma sources. The energy distribution of Sn particles varies from thermal to energetic. Thermal particles deposit on the EUV collector mirror surfaces and eventually lead to reduction of 13.5-nm reflectivity by absorption losses and variation of the surface morphology. Energetic particles, charged or neutral, coming from the expansion at the end of the pulse of the high-temperature pinched plasma induces sputtering and moderate surface roughness modification. Off-band radiation couples energy to the mirror in the form of heat where surface mirror temperatures can reach 200-400 °C, depending on geometrical mirror design and thermo-mechanical cooling system. Understanding the effect of Sn particles on EUV reflectivity performance is central to determine collector lifetime for Sn-based EUVL sources. Other EUVL sources use Xe as the radiator fuel. In this case Xe plasma also generates both charged and neutral species with a given energy distribution. For Xe-based LPP configurations, fast Xe ions have been measured to have average kinetic energies of 1-3 keV or higher [1,2]. However, these energies can be mitigated with the use of flowing or static gases slowing the particles down to energies below 1-keV.

Damage to VUV, EUV, and X-ray Optics, edited by Libor Juha, Ryszard H. Sobierajski, Hubertus Wabnitz
Proc. of SPIE Vol. 6586, 65860W, (2007) · 0277-786X/07/$18 · doi: 10.1117/12.723692

Contamination and lifetime of the collector optic used in EUVL sources depends on the configuration used to generate the EUV light. For example, in LPP-based sources multi-layer mirrors (MLM) are utilized since the collection angle is near normal to the optical surface. In contrast, single-layer mirrors (SLM) are used in DPP-based systems since the collection of light needs to be compatible with the forward pinch generated in DPP systems. Both fast Xe and Sn particles (ionized and neutral) can induce mixing and erosion at the surface of optical mirrors used. Both Xe and Sn are considered heavy-ions (atoms) and implantation at low-keV energies and below are dominated by the nuclear collision stopping cross-section effectively stopping the energetic implanted particles few ML from the air/film interface. Over large fluences however, ion-mixing effects coupled to prolonged sputtering can induce damage in several nm in depth. This can be particularly damaging to the first few bilayers used in typical MLM systems with a thickness of approximately 6-7 nm [3].

In addition to applications in EUV lithography, the results presented in this paper also have important ramifications in the area of X-ray astronomy. Grazing incidence (GI) mirrors are typically used to image the X-ray spectrum using grazing incidence telescopes with Wolter I type (parabolic-hyperbolic) mirrors. These mirrors also are exposed to a plethora of debris and thus understanding how various radiation (charged-particles, photons, etc…) affect optical properties is vital. In addition, GI optical mirrors used for X-ray astronomy GI telescopes also utilize multi-layers for focusing of soft X-ray light. Thus, the results in this paper of fast particle irradiation on both GI thin-film mirrors and MLM systems are relevant.

2. EXPERIMENTAL SETUP

2.1 In-situ surface characterization in IMPACT

The Interaction of Materials with Particles and Components Testing (IMPACT) experimental facility has been described in earlier publications and one to be published soon [4,5]. We briefly describe it here and elaborate briefly on the *in-situ* EUV reflectometry system used for some of the results presented in this paper and in previous work. Figure 1 shows a schematic of the IMPACT experimental facility. IMPACT uses a number of ion sources providing mirror exposure to irradiation of fast particles. Changes induced by the energetic particles can be diagnosed by several techniques including EUV reflectivity. The EUVR system in IMPACT was designed to measure the relative at-wavelength (13.5-nm) reflectivity performance of candidate SLM samples during exposure to either or both thermal and energetic particles. For application to EUV lithography at 13.5-nm Sn and Xe are studied since these are used as 13.5-nm radiation fuels.

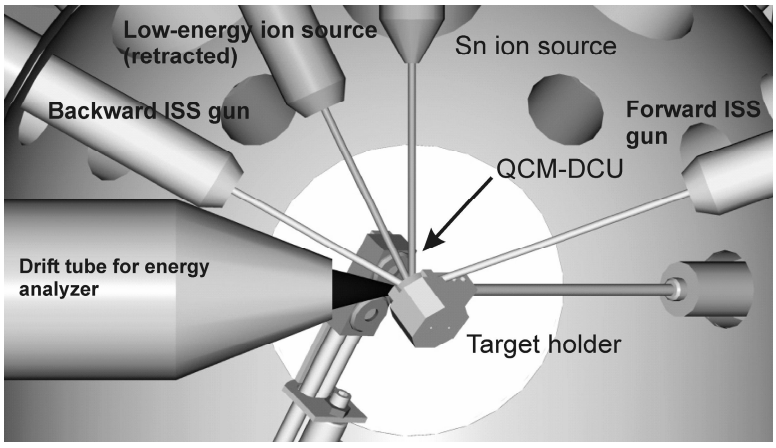

Figure 1: Schematic of relative positions of ion sources, target holder, QCM-DCU and energy analyzer drift tube. Sample in 45-degree incidence tilt and low-energy gun is retracted. Actual work distance of low-energy ion source is about 35 mm.

IMPACT is a UHV system where base pressures between 10^{-9} and 10^{-7} mbar are routinely achieved. IMPACT uses several in-situ metrology techniques that are able to measure the local surface atomic concentration of implanted or deposited Sn atoms during either exposure to ions or thermal atoms, respectively. In-situ techniques include low-energy ion scattering spectroscopy (LEISS), Auger electron spectroscopy (AES), X-ray photoelectron spectroscopy (XPS) and extreme ultraviolet photoelectron spectroscopy (EUPS). All these techniques can interrogate the sample during exposure. The partial pressures of the background gases in the system during the experiments are monitored with a residual gas analyzer and typical values are listed in Table 1.

Another particular strength of the IMPACT experimental facility is its ability to expose mirrors to a *combination* of irradiation sources. This aids in the ability to effectively simulate conditions in a EUVL source device. For example, EUVL sources generate fast ions and neutral fuel particles (e.g., Sn and Xe) but in addition background Ar gas used to slow down these fast particles is excited by soft X-ray radiation creating dilute plasma on the mirror. Therefore both energetic heavy-atom particles and low-energy Ar ions can bombard the mirror surface. This combination can be studied in IMPACT with the addition of an evaporative Sn source for the case of condensable metal vapor inside EUVL source devices.

Table 1: Background partial pressures in the IMPACT main chamber. Partial pressures measured with an Inficon L100 residual gas analyzer using a quadrupole mass spectrometer.

Gas	partial pressure [mbar]
water	5×10^{-9}
nitrogen	5×10^{-10}
oxygen	1×10^{-10}

The ion beam source for our experiment is a 1402A electron impact ionization gun from Nonsequitur Technologies, designed for inert gasses at low energy in the energy range between 10 and 1000 eV. It is capable of delivering up to 1 μA of current to the target with current densities of 3-30 $\mu A/cm^2$ for projectile energies in the range of 30-100 eV. Beam intensities are controlled by selecting the energy, filament emission current, and extractor and lens voltages. For ion beams of energy greater than ~ 200 eV, imaging is possible on a Li_2O sample surface by ion-induced photoemission of 540 nm light.

The system is further equipped with an electron gun, ion gun, X-ray source and PHOIBOS MCD 100 hemispherical energy analyzer to provide in-situ surface analysis diagnostics such as Ion Scattering Spectroscopy (ISS), X-ray photoelectron Spectroscopy (XPS) and Auger Electron Spectroscopy (AES) to monitor the elemental and chemical state of the target surface eroded. When the target holder is retracted the total current of the ion beam can be measured with a Faraday cup. To monitor the beam current during the experiment the sample holder is connected to the ground through a Keithley picoammeter. There is also a quartz crystal microbalance that monitors the erosion rate *in-situ* during ion bombardment.

LEISS gives compositional information about the top monolayer in the sample, while AES and XPS probe the subsurface layers due to 1) probing depth of kinetic electrons in AES and 2) probing depth associated with emitted photoelectrons' depth range. The techniques complement each other and allow a more reliable identification of components as well as their relative abundance and chemical state. In-situ diagnosis of samples monitors dynamic changes that can occur on a surface during irradiation by an ion beam; for example, radiation-induced segregation may drive certain target components to the surface, while radiation-enhanced diffusion will drive them away from the surface. Such phenomena are usually very hard to study by looking at samples before and after the treatment, since the mere act of transporting them to a different chamber for analysis modifies the surface. In addition, the relative changes of Sn surface atom fraction are inherently connected to exposure dose and thus demanding in-situ diagnosis.

3. RESULTS AND DISCUSSION

3.1 Effect of surface roughness on 13.5-nm reflectivity

The effect of roughness on optical reflectivity at 13.5-nm spectral region largely depends on the configuration being used. In the case of grazing incidence mirrors of the Wolter I type light is collected efficiently at grazing incidence angles between 5-20 degrees, while elliptical type mirrors collect light at angles between 30-50 degrees or more [6]. Fig. 2 shows IMD simulation results of surface roughness (air/film interface) effect on 13.5-nm reflectivity of the candidate GI mirror material Pd. The specular reflectivity has a distinct relation with the air/film interface (surface roughness) assuming one can separate out the specular and diffusive scattering components of X-rays scattering from single layers [7]. The specular reflectivity, *R,* relation is namely:

$$R = \frac{16\pi^2 \rho^2 r_0^2}{q_z^4} \exp(-q^2\sigma^2) \qquad (3.1)$$

where, ρ is the electron radius, r_o is the scattering length, q_z is the wave vector component normal to the surface and defined as: $q_z = (4\pi/\lambda)\sin\theta$, where θ is the incident angle between the X-rays and mirror surface, σ is the surface roughness parameter. This relation is used in IMD simulations of the 13.5-nm reflectivity for various surface roughness values comparing Pd and Ru mirrors.

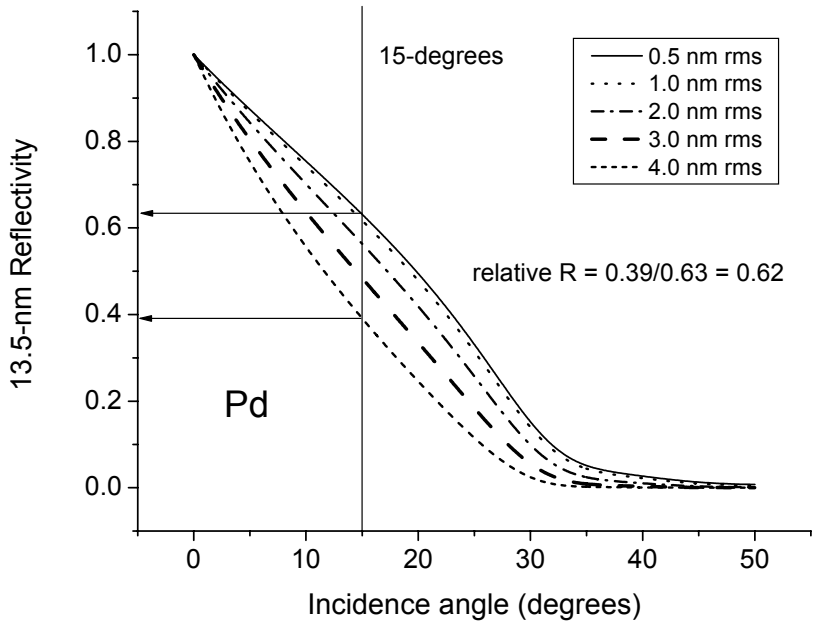

Figure 2: IMD Simulation of 13.5-nm reflectivity as a function of incident angle (with respect to mirror surface) for various air/film interface roughness values of a Pd GI mirror. Roughness is described by a root-mean-squared value corresponding to the height-height correlation function of a surface as measured by atomic force microscopy.

From Fig. 2, we find that for a Pd mirror with a surface roughness of 0.5-nm the absolute reflectivity at 15-degree incidence is about 0.63. The IMD simulation shows that in order to reach a substantial loss in reflectivity, the surface roughness must evolve up to values between 4-5 nm for losses near 40%. Since EUV power at the intermediate focus near the entrance of the illuminator in a EUV lithography stepper device is dictated by absolute reflectivity, any losses

greater than 10% must be avoided. Comparing to Pd mirrors results are obtained with IMD simulation for a Ru GI mirror and shown in Fig. 3. For the case of a Ru GI mirror the relative reflectivity is higher for the case of a 4-nm rms surface roughness value with a loss of 19% compared to almost 40% in the case of Pd GI mirrors.

In addition to this comparison another point is noted regarding surface roughness effect on 13.5-nm reflectivity. Previous experimental results on Ru GI *and* MLM mirror surfaces have shown that when exposed to energetic particles, the surface roughness does not increase beyond a 1 to 1.5-nm rms roughness value [3,8]. This is primarily due to the stepped microrelief (enhanced roughness) during sputtering of polycrystalline (PC) thin films being much less than solid PC metals due to relatively small grain size in thin films [9]. These results therefore suggest that irradiation-induced surface roughness enhancement and consequently reduction in reflectivity at 13.5-nm is less likely for GI thin-film mirrors. In the case of MLM mirrors used at normal incidence this is not necessarily true in that energetic particles can induce ion-mixing and interface roughness increase between bilayers, thus reducing reflectivity. For MLM architectures used at grazing incidence, energetic particles can also increase interface roughness but since the penetration depth is reduced the decrease is minimized.

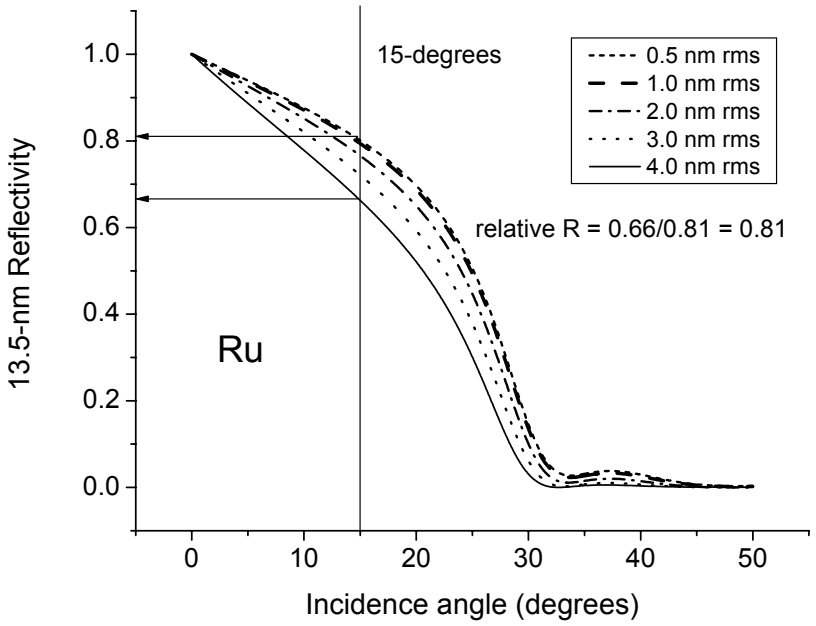

Figure 3: IMD Simulation of 13.5-nm reflectivity as a function of incident angle (with respect to mirror surface) for various air/film interface roughness values of a Ru GI mirror. Roughness is described by a root-mean-squared value corresponding to the height-height correlation function of a surface as measured by atomic force microscopy.

3.2 Effect of fast particles on MLM reflectivity at 13.5-nm

The effect of fast particle bombardment on MLM reflectivity at 13.5-nm and normal incidence is studied in this section. As mentioned earlier, energetic particles can induced interface roughness and thus reduce near-normal 13.5-nm reflectivity due to ion-induced mixing. Previous results have demonstrated this effect and only summarized here [3]. Xe^+ irradiations of Ru-capped and uncapped MLM systems for various fluences, two incident Xe ion energies (1-keV and 5-keV) and two sample temperatures: 298 K and 473 K were completed in previous studies.

For 1-keV Xe^+ and 298 K, peak reflectivities remain unchanged with fluences ranging in the order of 10^{14} to 10^{16} Xe^+/cm^2. These reflectivity measurements consisted of X-ray reflectivity using CuKα light and in particular used the 1st diffraction peak. For bombardment with 5-keV and 473 K conditions, the reflectivity response decreased, even at fluences of the order of 10^{14} Xe^+/cm^2. At very high fluences, > 10^{17} Xe^+/cm^2 at 1-keV and 298 K, the MLM surface showed signs of blistering. Low fluence exposures below ~ 5×10^{14} Xe^+/cm^2, had sputter rates of about 0.001 Å/sec.

For moderate fluence levels between 5×10^{14} and about 5×10^{16} Xe^{+}/cm^{2}, sputter rates average about 0.06 Å/sec. And at high fluence levels > 10^{17} Xe^{+}/cm^{2}, sputter rates reach near 2.0 Å/sec.

In addition to erosion regimes discovered with IMPACT experiments of MLM, a synergistic mechanism between high temperature exposure (up to 473 K) and ion irradiation was also discovered. Samples that were heated *and* irradiated suffered a loss in X-ray reflectivity for Xe^{+} bombardment at 1-keV. Control samples with heating alone, demonstrated that higher decrease in reflectivity is obtained when both heating and irradiation are applied to the MLM.

Surface analysis also concluded that surface roughness alone was not sufficient to qualify the performance of the mirror. In fact, erosion rates alone were not sufficient as well. X-ray reflectivity analyses that look for interface mixing, in the case of MLM samples, were able to determine the effect of energetic heavy-ion irradiation on EUV reflectivity. In particular variations in atomic scale roughness, for example, increase in surface roughness from 0.2-nm RMS roughness up to 1.0-nm RMS roughness did not show any measurable effect on EUV reflectivity response of the mirror.

Another important result consisted of large dose Xe^{+} irradiation exposures that lead to near-surface blistering due to noble gas implantation. XRR results demonstrated that high fluence Xe^{+} exposures led to both surface blistering and cratering severely damaging the MLM. Any mirror exposed to fluences higher than 10^{17} Xe^{+}/cm^{2} would be damaged permanently. With the collector mirror lifetime for high-volume manufacturing (HVM) specified to operate between 10,000-30,000 hours; the limiting ion flux to the mirror is at most in the order of 10^{8} $Xe^{+}/cm^{2}/sec$. This limit is to prevent permanent loss of collector mirror performance regardless of cleaning systems. Current ion fluxes are known to be of the order of 10^{15}-10^{17} $ions/cm^{2}/sec$ without debris mitigation for moderate EUV power sources. This places a tremendous burden on debris mitigation and collector optics design.

3.3 Effect of multiple sources on surface chemistry and 13.5-nm reflectivity

Another radiation-induced damage concern in EUV (13.5-nm) lithography source devices is the existence of a radiation driven plasma near the collector optics. The radiation generates weakly-ionized plasma by photo-ionization of the argon background gas. Collisions of 92-eV photons with neutral Ar gas atoms generate a fast electron at a kinetic energy of about 76 eV and a slow Ar ion with energy below 50 eV. Ions can be accelerated in the plasma sheath towards the first condenser optic (collector mirror), potentially causing damage through physical sputtering. In addition, low-energy Ar ions can induce physical etching mechanisms, which in synergy with both thermal Sn atoms and energetic fast Sn ions can lead to an equilibrium kinetic state whereby the EUV reflectivity can be affected. IMPACT was used to study the effect of the synergy between these various sources of damage on the collector optical surface.

Three sources of debris were selected in IMPACT to study the effect on at-wavelength EUV reflectivity in real time. The first was a source of thermal Sn atoms simulating the expanding Sn plasma in a Sn-DPP or Sn-LPP source. The second was the use of 1-keV Xe ions to simulate the condition of fast heavy-ions such as Sn. The last was using the low-energy ion source generating 100 eV Ar ions for bombardment. During exposure to the thermal source and two energetic sources the surface was characterized with LEISS and XPS. In addition the mirror EUV reflectivity was monitored in-situ and in real time during exposure.

Typical LEISS and XPS spectra obtained with Ru target exposed with various levels of Sn fluence are given in figure 4. For comparison, the XPS and LEISS spectra obtained from a virgin Ru sample are also shown in the figure. During this experiment, along with thermal Sn, the Ru target was simultaneously irradiated with 1keV Xe ions and 100eV Ar ions. The peaks in the XPS spectrum corresponds to the photo-ionization of the inner electron shells of the elements present in the surface of the sample. Various photoelectron peaks observed in the XPS spectra are assigned using literature and also given in figure 4. Atomic content of the different elements was determined by analyzing the XPS spectra with the CASA software package. All scans consistently show C and O present in the sample, and the calculated atomic fractions are done considering only the Ru and Sn 3d photoelectron lines. The estimated Ru and Sn fractions obtained from XPS spectra analysis are shown in figure 5. The atomic fraction obtained from LEISS spectra also given in the same figure.

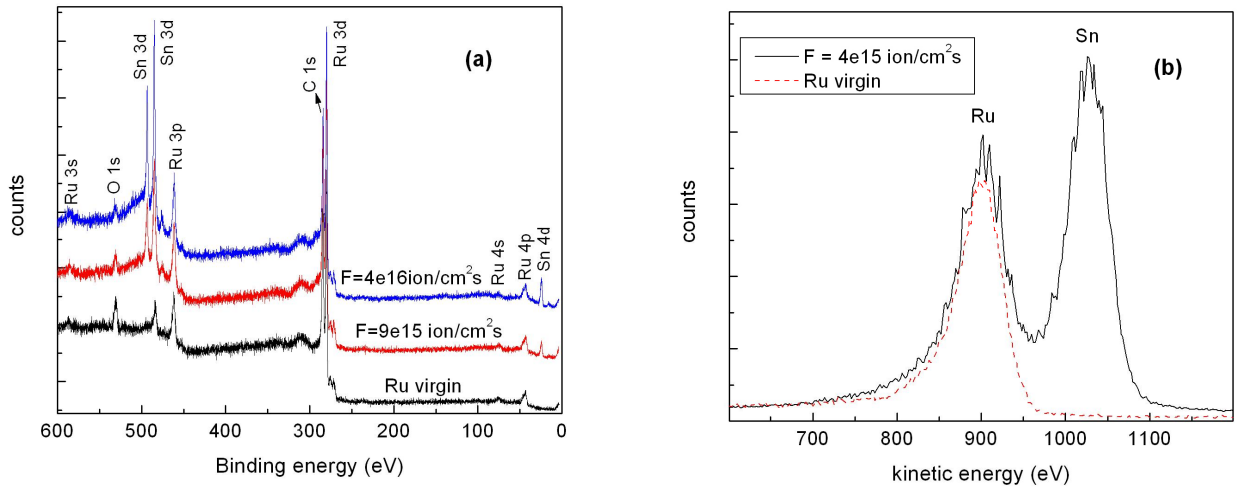

Figure 4: (a) XPS spectra obtained from Ru sample with various thermal Sn exposure levels. The spectrum obtained with Ru virgin sample is also given. (b) LEISS scan taken with 2keV Ne^{+} for virgin Ru and thermal Sn exposed Ru.

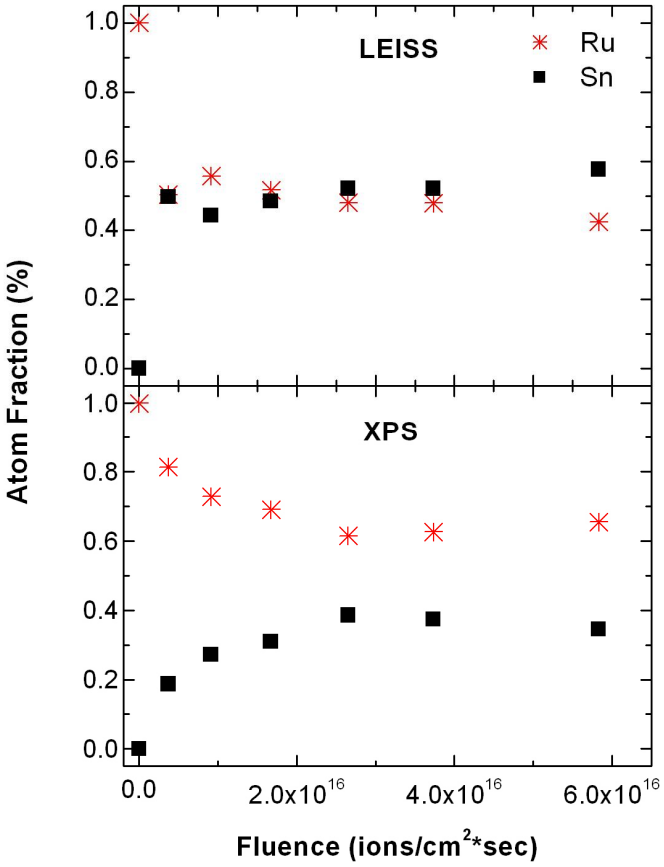

Figure 5: The atom fraction for Sn and Ru obtained from LEISS and XPS spectra.

The quantitative analysis of LEISS spectra showed that the Sn fraction becomes 50% even with lowest Sn thermal fluence levels used in the experiment and saturates at higher levels of thermal Sn deposition. In contrary, the Sn atomic

fraction estimated with XPS data showed gradual increase with thermal Sn fluence until exposed Sn thermal flux levels of 2.5×10^{16} ions $cm^{-2}s^{-1}$ and found to be constant thereafter. It is important to recall that LEISS provides compositional information about the top monolayer in the sample, while XPS probes the subsurface layers due to the probing depth associated with emitted photoelectrons' depth range. This result is very important in that a spatial dependence of the Sn inventory as a function of depth is measured between LEISS and XPS results. These results conclude that most of the Sn remains in the top 1-3 nm of the mirror surface.

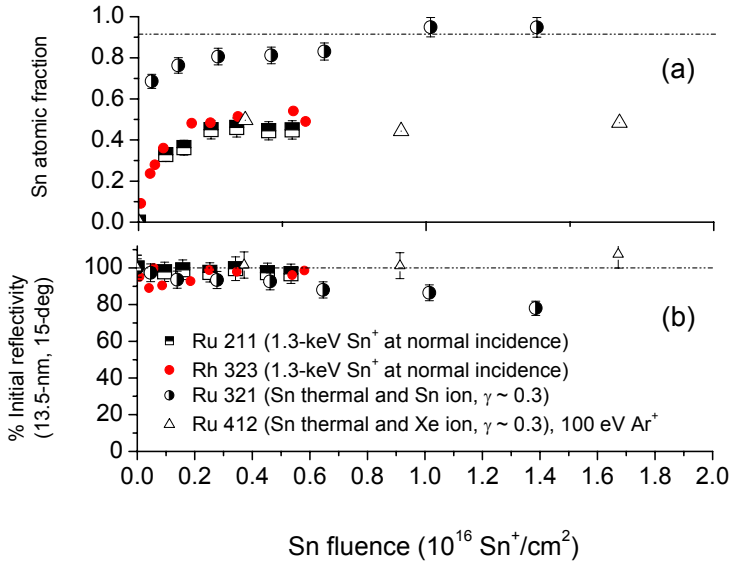

Figure 6: (a) LEISS data of Sn surface atomic fraction for Ru and Rh mirrors exposed to various exposure conditions including mixed thermal Sn and energetic beams (i.e. Sn, Xe and/or Ar) (b) Corresponding in-situ EUV at-wavelength reflectivity data.

Figure 6 shows LEISS Sn surface atomic fraction data for Ru 412 sample compared to another Ru mirror (Ru 211) and a Rh mirror sample (Rh 323). The Ru 311 and Rh 323 samples were both irradiated by 1.3-keV Sn^+ ions at normal incidence and at room temperature. An additional comparison is made to sample Ru 321, which was irradiated by both Sn ions and exposed to thermal Sn atoms. The ratio of ion flux to thermal flux for Ru 321 was the same as that used for Ru 412 sample and equal to 0.3. The results are very illuminating. First, for fluences up to 0.5-0.6 x 10^{16} cm^{-2}, the Sn surface atomic fraction reaches levels between 45-50% for all samples: Ru 211, Rh 323 and Ru 412. In the case of Ru 321 the fraction is higher at close to 90% as indicated by the dashed line in Fig. 6. This indicates that erosion from the synergy of Xe and Ar ions leads to sufficient Sn atom sputtering. Also, Ru 321 used Sn *ions* as well as a thermal source, while Ru 412 used Xe *ions* instead. Kinematically both Sn and Xe are identical. The goal with the experiment was to determine how important a role Xe played. In addition to Xe bombardment however Ar ions were also used. Therefore we expect that if Ar ions were not used, the Sn fraction would have been a bit higher level ~ 60%. Ar ions were used to simulate the condition of ionized Ar gas forming plasma at the collector mirror. Fig. 6 shows the effect the combined set of ion species have on the at-wavelength (13.5-nm) EUV reflectivity.

From this data it is very clear the correlation between the amount of Sn at the surface and the relative reflectivity loss. For the case of the Ru 321 sample, the surface Sn fraction equilibrates between 85-90% and its reflectivity is decreased by about 20% over a fluence of 10^{16} Sn^+ cm^{-2}. On the other hand, the Ru 412 case with an added energetic source in Ar, has no change (loss) in reflectivity and it coincides with a lower amount of Sn at the surface near 50% Sn. The optical mirror has sufficient Ru remaining to reflect the incident 13.5-nm photons.

4. SUMMARY AND CONCLUSIONS

Three main aspects of energetic and thermal particle exposure on SLM systems have conducted in the IMPACT experimental facility. These consisted of: 1) the effect of surface roughness on 13.5-nm reflectivity, 2) Effect of fast

particles on MLM reflectivity at 13.5-nm, and 3) Effect of multiple sources (energetic and thermal) on surface chemistry and 13.5-nm reflectivity.

The effect of surface roughness on 13.5-nm reflectivity was studied comparing IMD simulations to experimental data. For surface roughness values of 4-nm rms for a Pd mirror leads to a 13.5-nm reflectivity loss of about 40%. For the same surface roughness increase to 4-nm rms the reflectivity at 13.5-nm from a Ru surface decreases by about 20%. This difference may be due to the low Sn absorption properties of Ru compared to Pd. The surface roughness evolution measured for both MLM and SLM systems does not increase above 1-2 nm rms [3,8]. Therefore, surface roughness increase under energetic particle irradiation is expected to be moderate and consequently the decrease of 13.5-nm reflectivity to be negligible.

Energetic particles have a dramatic effect on MLM system primarily destroying the near-surface interface layers between dissimilar material bilayers. For fluences above 10^{14} Xe^{+} cm^{-2}, the interface damage leads to absolute reflectivity losses of greater than 10%. For fluences above 10^{16} Xe^{+} cm^{-2} lead to inert gas accumulation and stability of surface bubbles, which in turn decrease reflectivity due to an effective decrease in electron density at the surface.

Combined energetic sources of Ar and Xe bombarding the surface during Sn thermal atom exposure also leads to equilibrium conditions with about 50% Sn accumulation at the first monolayer of the SLM surface. Sputtering is dominant and reaches levels beyond unity sputtering. However, due to preferential sputtering of Sn atoms the rate of erosion is decreased and thus lifetime of the optical mirror increased. The 13.5-nm reflectivity does not decrease significantly even for fluences beyond 10^{16} # cm^{-2}. Further work will study the effect on various mirror system conditions including temperature and impurity coverage.

5. ACKNOWLEDGMENTS

We acknowledge helpful discussions with V. Banine of ASML and regarding EUV-induced plasma creation at EUVL source region near collector optics. We also acknowledge our collaboration with Peter Zink of Philips Extreme UV. This work was supported by Intel Corporation and in part by the U.S. Department of Energy under Contract DE-AC02-06CH11357. We thank Albert Macrander, Ray Conley and Chian Lu of the Optics Fabrication and Metrology Lab in the Advanced Photon Source at Argonne for fabrication of single-layer optical mirrors.

6. REFERENCES

1. H. Komori, Y. Imai, G. Soumagne, T. Abe. T. Suganuma, A. Endo; “Magnetic field mitigation for collector mirrors”, EUVL Symposium, 2004, Miyasaki, Japan.
2. K. Nishihara, “Modeling of LPP EUV Light Source at Japan MEXT Leading Project” EUVL Symposium, 2004, Miyasaki, Japan.
3. J.P. Allain, et al., “Xe^{+}-Irradiation Effects on Multilayer Thin-Film Optical Surfaces in EUV Lithography”. Nuclear Instrum. Methods B. 242 (2006) 520.
4. J.P. Allain, A. Hassanein, et al., “Effect of charged-particle bombardment on collector mirror reflectivity in EUV lithography devices”, Proc. SPIE Int. Soc. Opt. Eng. 6151 (2006) 31.
5. J.P. Allain, et al., *"Energetic Sn^{+} irradiation effects on collector mirror specular reflectivity in the EUV spectral range"*, Applied Phys Lett., To be submitted 2007.
6. E. Buratti, et al., “Optimisation of Optical Design in Grazing Incidence Collector for EUV Lithography DPP Sources,” EUVL Symposium, 2005, San Diego, USA.
7. M.K. Sanyal, A. Datta and S.Hazra, Pure Appl. Chem., Vol. 74, No. 9, 1553-1570, 2002.
8. M. Nieto, J.P. Allain, A. Hassanein, et al. “Effect on xenon bombardment on ruthenium-coated grazing incidence collector mirror lifetime for EUV lithography” J. Appl. Phys. 100 (2006) 053510.
9. S. Brongersma, J. App Phys. 86, 3642, 1999.